ELSEVIER

Thermochimica Acta 316 (1998) 57–73

thermochimica acta

The oxidation of calcium sulphite by calcium nitrate

Andrew K. Galwey[1,a,*], Clodagh Ettarh[b]

[a] *School of Chemistry, The Queen's University of Belfast, Belfast, BT9 5AG, Northern Ireland, UK*
[b] *Questor Centre, The Queen's University of Belfast, Belfast, BT9 5AG, Northern Ireland, UK*

Received 29 July 1997; received in revised form 20 January 1998; accepted 10 February 1998

Abstract

Crushed powder mixtures of calcium sulphite and calcium nitrate exhibit an exothermic reaction between 650 and 700 K. This rate process has been investigated by dynamic and isothermal DSC experiments, complemented with isothermal rate studies based on gas evolution in a vacuum apparatus, together with some product analyses. It is concluded that the overall reaction is complicated, including several concurrent contributing chemical changes, in which sulphite oxidation to sulphate is a dominant process, accompanied by some nitrate decomposition. On heating to higher temperatures (above 800 K) a second endothermic reaction was identified as the melting and breakdown of calcium nitrate. These processes occurred at temperatures somewhat less than those characteristic of the pure salt, possibly due to the presence of products from the first reaction including small amounts of $Ca(NO_2)_2$. The dominant exothermic reaction was accompanied by fusion, at temperatures significantly below the melting point of either reactant. This may be due to the intermediate formation of $Ca(NO_2)_2$, melting point 551 K, or the generation of liquid product following hydrolysis reactions with water evolved during dehydration of reactant $CaSO_3{\cdot}1/2H_2O$, with which the exothermic oxidation overlapped. This dehydration step was a precursor to sulphite oxidation. A detailed reaction mechanism is not proposed here due to the difficulties of separating the contributions from the several probable concurrent participating reactions. The role of the fluid reactant believed to be active in the oxidation process, and containing NO_3^-, NO_2^-, SO_3^{2-} and possibly SO_4^{2-}, in desulphurization processes, is discussed as a possible route towards removing the precursors to acid rain from coal combustion emissions. It is known that $CaCO_3$ reacts with NO_x to form $Ca(NO_3)_2$. The present work identifies the liquid medium recognized in the exothermic reaction as enabling the oxidation of $CaSO_3 \rightarrow CaSO_4$ to proceed to completion at a lower temperature than the slow and product-opposed reaction of $CaSO_3$ with oxygen gas. Aspects of the chemistry of this complicated reaction and its potential value in pollution abatement are discussed.

1. Introduction

The wide dispersal of the precursors to acid rain that result from the gaseous emissions from power stations has been generally accepted as the direct cause of significant damage to the environment. Unrestricted anthropogenic releases of oxides of sulphur (SO_x) and of oxides of nitrogen (NO_x) into the atmosphere have demonstrably imposed stress on trees in forests, locally severe, caused fish kills in lakes and aquatic vegetation death, together with accelerated weathering of architectural materials. Widespread concern about the adverse consequences of acid rain has led to the introduction of controls that restrict the quan-

*Corresponding author. Tel.: +8001232 611459

[1]Present address: 18 Viewfort Park, Dunmurry, Belfast BT17 9JY, UK.

0040-6031/98/$19.00
PII S0040-6031(98)00305-0

tities of specific pollutants that are permitted in the gaseous effluents released from large-scale combustion plants. Recent attention has been most particularly concerned with SO_x releases and, in some large electricity generating plants, emissions require desulphurization to achieve tolerable levels. Much less progress has been made towards denitrification (NO_x removal). In some furnaces nitrogen oxide formation is minimized during the combustion process by the use of specialized burners whereby the supply of air admitted to the combustion zone is controlled in a series of successive stages. These different approaches are used because sulphur is a constituent of all coal fuels whereas the greater proportion of NO_x is formed during reactions of air (between N_2 and O_2) at high combustion temperatures.

Remedial action designed to reduce the release and, therefore, the consequences of unrestricted dispersal of pollutants into the atmosphere is, almost invariably, most effectively implemented within the generating plant. The recent introduction of controls is often seen as an unwelcome, imposed burden on the potential polluter, who may not himself obtain direct benefits from the costs of cleaning the emissions. Additional costs may be particularly unwelcome when these have not been levied in the past. Consequently, to be acceptable both to industry and to the public, the development of techniques introduced to maintain and to safeguard the health of our environment must be demonstrably the most effective and efficient that can be devised. Acid rain prevention, however, remains a problem of important topical interest.

The removal of sulphur oxides from power station gaseous effluents [1,2] has been supported by detailed mechanistic studies undertaken to identify the rate controlling processes in the sulphation reaction, which is represented by:

$$CaCO_3 + SO_2 + \tfrac{1}{2}O_2 \rightarrow CaSO_4 + CO_2 \qquad (1)$$

This approach is based on the relatively cheap reactant calcite (alternatively CaO and/or $Ca(OH)_2$ may be used). The SO_2 is converted into an inert product, $CaSO_4$, for disposal in a land-fill site or alternatively it can be treated to manufacture more valuable commercial products, such as gypsum ($CaSO_4{\cdot}2H_2O$ is used in plaster board), elemental sulphur or sulphuric acid.

In contrast, there is very much less information available concerning the chemical properties of nitrogen oxides, reactants that may possibly participate in reactions of calcite during flue-gas desulphurizations. It is known [3–6] that under suitable conditions NO and NO_2 can react with $CaCO_3$ to form $Ca(NO_3)_2$. We considered it to be of interest to undertake further studies of the thermal reactions of $Ca(NO_3)_2$ that may be relevant to flue-gas desulphurization processes for two main reasons. Firstly, there is the possibility that calcite could be used for flue-gas denitrifications if, in the future, this becomes necessary. Secondly, oxides of nitrogen may participate in those desulphurization reactions where $CaSO_3$ is a probable intermediate, Eq. (1)[1,2,7]. We have, therefore, undertaken a research programme intended to investigate the possible and potential roles of $Ca(NO_3)_2$ in flue-gas treatments with calcite. Previous publications from this initiative have been concerned with the decomposition of $Ca(NO_3)_2$ alone [3] and catalyzed by a range of metal oxides [8]. While these results have chemical and mechanistic interest, it was accepted that a major objective of the work, to identify a route whereby the oxidized nitrogen in the anion (NO_3^-) could be converted into environmentally benign products (preferably N_2 and O_2) was not realized.

The study reported here is concerned with a possible alternative route for the removal of NO and NO_2 from flue gases through reactions with calcite to form $Ca(NO_3)_2$ which may then oxidize $CaSO_3$. The present results show that the isothermal reaction of $Ca(NO_3)_2$ with $CaSO_3$, identified as yielding $CaSO_4$, proceeds by an apparently autocatalytic fractional reaction (α)–time rate process [9] between 660 and 700 K. Microscopic examinations of partly reacted mixtures gave textural evidence to indicate that these reactions proceed with the intervention of a liquid phase. This was unexpected because $Ca(NO_3)_2$ melts at 836 ± 2 K [3] and the melting point of $CaSO_3$ is known to be above 850 K, but has not been measured because of salt breakdown [7]. The participation of a melt is, however, of interest and potential value as a method of avoiding the inhibiting effect of the comprehensive and strongly adherent barrier layer that opposes the sulphation reaction (1), thereby preventing it from proceeding to completion [1,2,7]. The present observations are, therefore, regarded as promising and may indicate potentially profitable

directions for future investigations of methods for the removal of the nitrogenous precursors to acid rain from flue gases. The mechanisms of the reactions between calcium nitrate and calcium sulphite are discussed below and their possible value in contributing to pollution abatement is considered.

2. Experimental

2.1. $Ca(NO_3)_2$+$CaSO_3$ reactant mixtures

Eight reactant mixtures, having the compositions specified below, were prepared by an identical procedure. The constituents of each reactant mixture were weighed in sufficient quantity to enable completion of each set of experiments using a single batch. Individual mixtures were thoroughly crushed together using a pestle and mortar. The constituent salts used in the present reactants were as follows.

$Ca(NO_3)_2 \cdot xH_2O$: BDH anhydrous calcium nitrate. This compound is hygroscopic and before use had rehydrated to a small extent during brief exposures to the atmosphere.

$Ca(NO_3)_2$: Samples of the previous reactant were redehydrated 30 min at 460 K immediately before reactant mixture preparation and thereafter protected from atmospheric moisture.

$CaSO_3 \cdot 1/2H_2O$: This reactant was supplied by Pfaltz and Bauer (for research use), and used in previous studies [10].

$CaSO_3$: The previous reactant was dehydrated for 60 min at 650 K in vacuum [10] and protected from rehydration.

Mixtures A–D were prepared from $Ca(NO_3)_2 \cdot xH_2O$ and $CaSO_3 \cdot 1/2H_2O$ (above) in molar ratios 1.0 : 0.7(A), 1.3(B), 2.5(C) or 2.6(D). For convenience, the reference in each mixture label mentions the molar ratio of $CaSO_3$ to 1.0 mol $Ca(NO_3)_2$, e.g. Mixture A (0.7), Mixture B (1.3), etc. Mixtures W–Z were similarly prepared from the anhydrous reactants in molar ratios $Ca(NO_3)_2$ 1.0 to $CaSO_3$ W (0.6), X(0.9), Y (0.9) and Z (1.0).

2.2. Differential scanning calorimetry

A Perkin–Elmer DSC7 instrument was used throughout the present work. All data were recorded in the memory of an IBM PS2 computer using the DSC Standard and DSC Isothermal software supplied by Perkin–Elmer. Reactant samples were weighed on a Mettler MT5 balance directly in the gold pan container. These were covered with a gold lid to promote thermal contact and to prevent losses by decrepitation. A matched gold pan and lid was always present as a reference. A flow of dry nitrogen (or air, as specified below) at 30 cm^3 min^{-1}, was maintained throughout all experiments. Response temperatures for the instrument were recalibrated at intervals using indium and zinc metal melting-point standards.

The principal source of uncertainty throughout all the DSC measurements was the position of the baseline, particularly in those reactions which involved gas evolution. All calculations were based on the software as supplied by Perkin–Elmer. For kinetic analyses of isothermal rate processes, the approximately horizontal traces before and after reaction were joined by a straight line and the displacement due to the response peak was used as a measure of reaction rate.

2.3. Vacuum gas-evolution experiments

Isothermal kinetic studies of the gas-evolution reactions were carried out in a conventional glass vacuum apparatus. After evacuation for 30 min at 10^{-4} torr, the weighed (40.0±0.1 mg) reactant sample, contained in a small glass vessel, was admitted to the heated reaction zone, maintained at constant temperature, ±1 K. The pressure of gas evolved in the apparatus was measured at prespecified time intervals by a MKS Baratron absolute pressure gauge, MKS222B, working in the range 0–10 torr and read ±0.001 torr. This was recorded automatically. Pressure–time data were stored in the computer memory for later analysis [1,7,10,11].

Volumetric gas-evolution experiments were completed at low pressure (below 10 torr) and without cold traps. A partial analysis of the volatile products was, however, achieved based on measured pressure changes resulting from the introduction of cold traps. *Liquid nitrogen* (78 K): N_2 and O_2 remain volatile and the vapour pressure of NO is ca. 0.2 torr [12]. *Liquid/solid acetone* (178 K): N_2, O_2, N_2O and NO are volatile. *No trap* (290 K): all expected products: N_2, O_2, N_2O, NO, NO_2 and H_2O, will contribute to the pressure (N_2O_4 is expected to be effectively comple-

tely dissociated at these low pressures, 2–3 torr. NO reacts rapidly with oxygen, $2NO+O_2 \rightarrow 2NO_2$).

3. Results and discussion

3.1. Rising temperature DSC studies

3.1.1. Mixture B(1.3)

The novel feature observed in preliminary DSC traces (10 K min^{-1}) for this mixture from 570 to 1000 K was a pronounced exotherm at ca. 700 K. This feature was absent from the traces observed for components of the mixture heated individually, which showed endothermic responses only, Fig. 1. As reported previously [3], $Ca(NO_3)_2$ melts with a sharp endotherm at 836±2 K and subsequent decomposition occurs at ca. 950 K, characterized as an irregular and somewhat overlapping series of endotherms, Fig. 1, Trace A. $CaSO_3 \cdot 1/2H_2O$, Trace C in Fig. 1, gave a single broad endotherm, maximum at 686 K, identified as hemihydrate dehydration [10]. No later responses attributable to $CaSO_3$ dissociation and/or decomposition were detected [7].

A typical response pattern for Mixture B (1.3) is shown in Trace B in Fig. 1. This results in the working hypotheses presented below, based on preliminary observations for this reactant, that provided the stimulus for us to undertake the overall investigation now reported. The exotherm is identified as a reaction between nitrate and sulphite in the mixture. From detailed examinations of the traces we concluded that the relatively rapid heat evolution reaction is usually preceded by and sometimes followed by endotherms, though the latter is not always discerned. Consideration of possible reactions in the mixtures (Ca^{2+}, NO_3^-, $SO_3^=$, together with some water) lead us to conclude that the only realistic heat-evolving process is sulphite oxidation to sulphate.

3.1.1.1. Working hypothesis. The exotherm (at ca. 700 K) is followed by endotherms in the vicinity of the temperature of $Ca(NO_3)_2$ melting. These are ascribed to the breakdown of that proportion of the nitrate that did not contribute to sulphite oxidation. Here, 2.0 moles of NO_3^- contain more oxygen than is required to oxidize the 1.3 mol of $SO_3^=$ ($\rightarrow SO_4^=$) present in this mixture. Decomposition of this

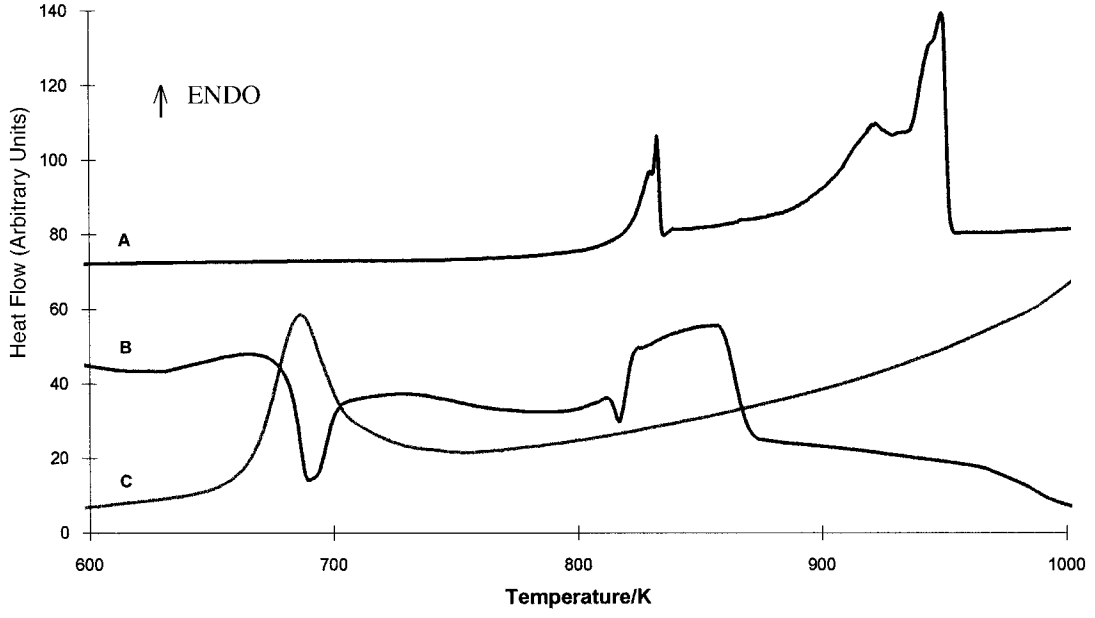

Fig. 1. Comparison of typical DSC response traces for reactions under identical conditions for (A) $Ca(NO_3)_2 \cdot xH_2O$, melting and decomposition, (B) Reactant Mixture B (1.3) of $Ca(NO_3)_2 \cdot xH_2O$ and $CaSO_3 \cdot 1/2H_2O$ and (C) $CaSO_3 \cdot 1/2H_2O$ dehydration. Heated at 10 K min^{-1} in N_2 flow at 30 cm^3 min^{-1}. For explanation see text.

excess $Ca(NO_3)_2$ is preceded by melting (a sharp endotherm is detected in most DSC traces) and is completed at relatively lower temperatures (ca. 890 K) than the pyrolysis of the pure salt (usually completed by 960 K). The appreciable diminution of the temperatures of both melting and anion breakdown are ascribed to the presence in the residual mixture of products remaining from the exothermic reaction and these very probably include $Ca(NO_2)_2$.

Quantitative comparative studies were made of heating Mixture B (1.3) at 5, 10 and 20 K min^{-1}, typical response traces are shown in Fig. 2. The mean position of the exotherm peak maximum (676, 690 and 703 K, all ± 1 K, for heating at 5, 10 and 20 K min^{-1}, respectively) increased systematically with heating rate, consistent with the view that this is an activated chemical reaction. Each trace usually included a subsequent sharp endotherm, identified as the onset of melting (often 812–826 K) but were always just below the melting point of pure $Ca(NO_3)_2$ (836$\pm$2 K). This is ascribed to contributions due to products retained from the oxidation reaction, accounting for the variations in peak shapes between successive, nominally identical experiments. Careful comparisons of the response traces for this mixture in air with those in N_2 identified no significant differences in any aspect of behaviour (Traces B and D in Fig. 2).

3.1.2. Mixture C(2.5)

A typical response trace is shown in Fig. 3 for this reactant mixture heated at 10 K min^{-1}. The pattern of behaviour is generally similar to that described for Mixture B (1.3) above but the following difference are identified as being significant. The exotherm peak occurs at virtually the same temperature (691 K) as for Mixture B (1.3) but is relatively larger. The minor endotherms before and after the exotherm are relatively more pronounced, extending between 653 and 733 K. This is ascribed to a greater thermal contribution resulting from the relatively larger proportion of $CaSO_3 \cdot 1/2H_2O$ in this reactant. Endotherms attributable to the melting and decomposition of $Ca(NO_3)_2$ are here relatively much reduced and completed at a lower temperature, 853 K. This is satisfactorily explained by the stoichiometric requirement that a greater amount of nitrate is required to oxidize the increased proportion of sulphite present here. The response traces obtained on heating this reactant at 5 and 20 K min^{-1} gave responses at temperatures that were closely similar to values for Mixture B (1.3), but again with the same modified pattern of behaviour as described above. Reaction in an air atmosphere was indistinguishable from that in N_2.

Responses observed for the second preparation, Mixture D (2.6), having a marginally different composition, gave peaks that agreed, within experimental error, with those of Mixture C (2.5).

3.1.3. Mixture A (0.7)

The exothermic response for this mixture was comparatively small, as expected from the reduced amount of sulphite present, a typical trace is shown in Fig. 4. Also, consistent with the pattern described in the previous paragraph, the associated endotherms were less evident. In contrast, responses due to $Ca(NO_3)_2$ melting and decomposition were relatively larger and more widely separated (compared with Mixtures B (1.3) and C (2.5)). These endotherms occurred at temperatures below those characteristic of the pure salt, but the influences from the residual products of the first reaction were noticeably less. The patterns of DSC response traces were, in all respects, closely similar to the behaviour described for the other mixtures containing the same reactants.

3.1.4. Mixtures A(0.7), B(1.3), C(2.5) and D(2.6)

For reactants of all four molar ratios, the mean peak temperatures of the exotherm were determined as 676, 691 and 703 K (± 1) for heating rates of 5, 10 and 20 K min^{-1}, respectively. No significant differences in response patterns could be discerned between reactions in N_2 and in air. Thermochemical data are summarized in Table 1 and Fig. 5.

3.1.5. Mixtures W(0.6), X(0.9), Y(1.0) and Z(1.0)

Samples of these reactants containing anhydrous $CaSO_3$ were heated in the DSC apparatus under conditions identical to those described above. The pattern of behaviour recorded was generally similar but with the following significant differences. The reaction exotherm was again present but occurred at a temperature that was $+11\pm1$ K higher than those characteristic of mixtures containing the hydrated salt, for example at 702$\pm$1 K when samples were heated at 10 K min^{-1}. The endotherms associated with this response were absent confirming that this feature

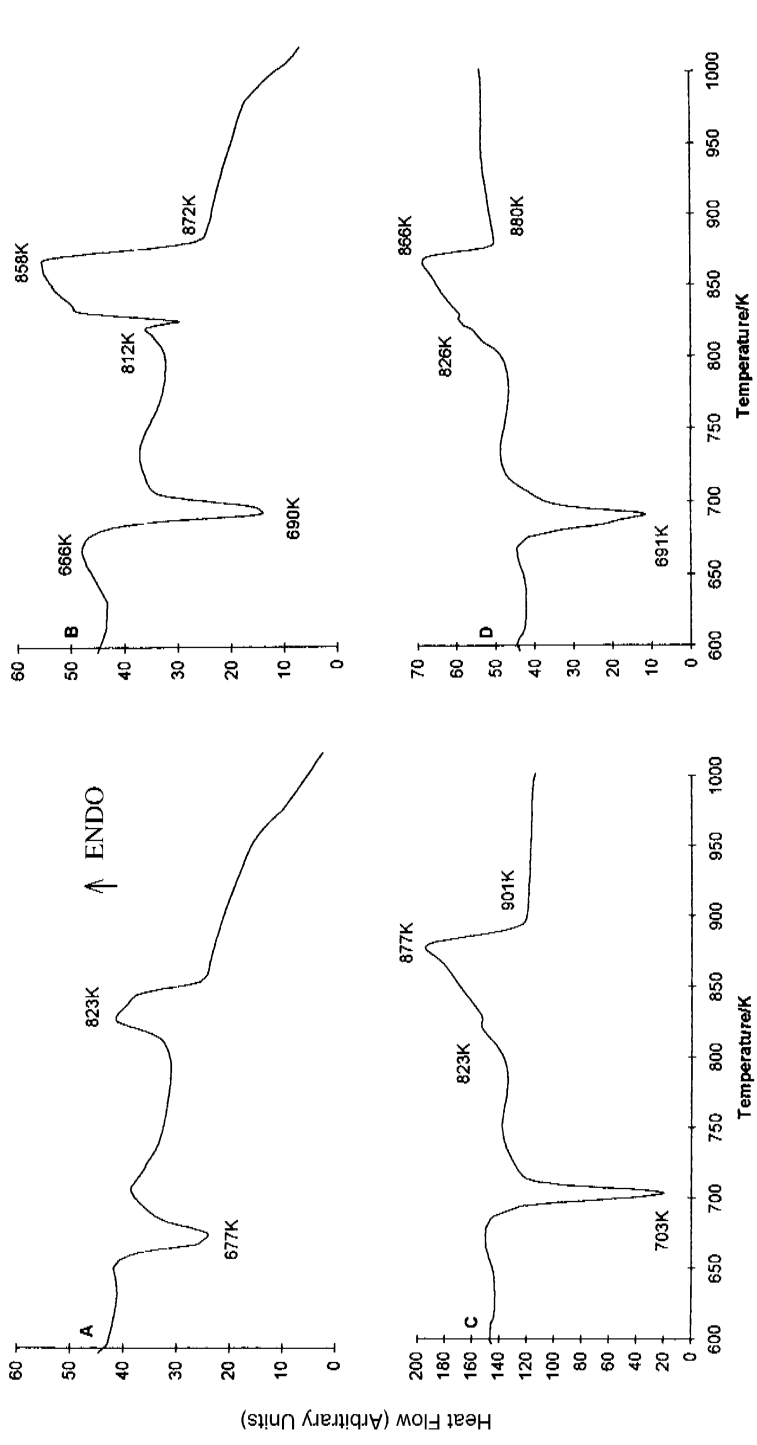

Fig. 2. Typical DSC response traces for reaction of Mixture B (1·3) on heating at (A) 5, (B,D) 10 and (C) 20 K min^{-1} in (A,B,C) N_2 and (D) air flowing at 30 cm^3 min^{-1}.

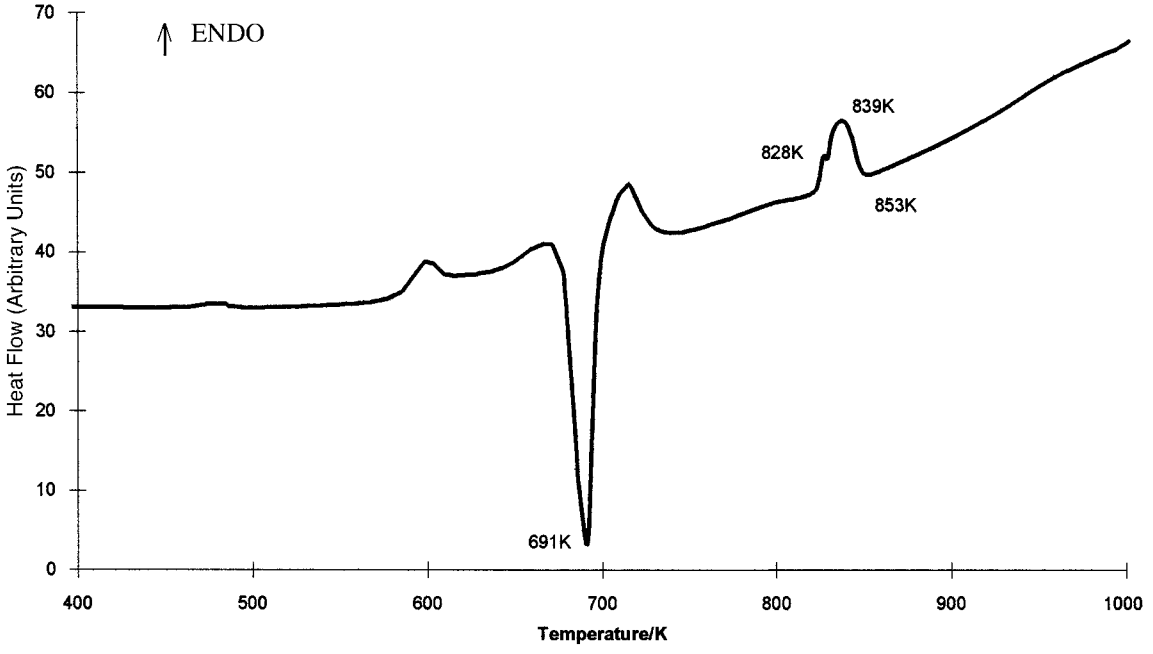

Fig. 3. Typical DSC response for Mixture C (2.5) on heating at 10 K min^{-1} in N_2.

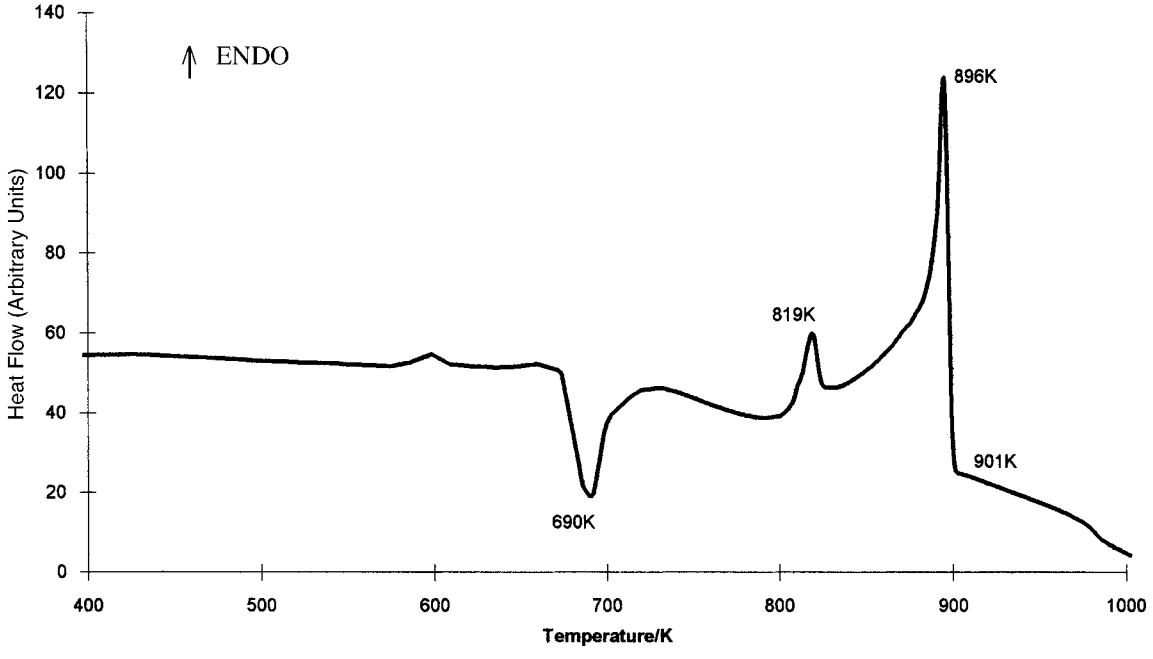

Fig. 4. Typical DSC response for Mixture A (0.7) on heating at 10 K min^{-1} in N_2.

Table 1
Summary of thermochemical data from DSC studies of decompositions of various crushed reactant $Ca(NO_3)_2$+$CaSO_3$ mixtures

Mixture	Molar composition		Enthalpy of exotherm (maximum at 691 K for 10 K min^{-1})		Enthalpy of combined response melting and decomposition	Nitrate reacting[a] in the exothermic process
	NO_3^-	$SO_3^=$	kJ(mol $CaSO_3$)$^{-1}$	kJ(mol $Ca(NO_3)_2$)$^{-1}$	kJ (mol $Ca(NO_3)_2$)$^{-1}$	mol($Ca(NO_3)_2$)$^{-1}$
A(0.7)	2.0	0.7	−71±8	−49±5	374±13	0.68
B(1.3)	2.0	1.3	−65±9	−92±13	243±21	1.12
C(2.5)	2.0	2.5	−77±3	−211±9	53±7	1.82
D(2.6)	2.0	2.6	−61±9	−167±25	82±1	1.72
X(0.9)	2.0	0.9	−37±3	−32±2	375±6	0.68
Z(1.0)	2.0	1.0	−28±2	−53±4	464±44	0.36
$CaSO_3$	0	1.0	+52±5	—	—	—
$Ca(NO_3)_2$	2.0	0	—	—	568±31	0

[a] Number of moles of nitrate participating in the exothermic process were calculated from the original reactant composition and subtraction of the amount of calcium nitrate melting and decomposing in the higher temperature range (above 800 K) estimated from the area of the total composite endotherm.

resulted from $CaSO_3 \cdot 1/2H_2O$ dehydration [10]. The subsequent endotherms ascribed to $Ca(NO_3)_2$ melting and decomposition were quantitatively similar in all respects to the hydrate containing mixtures and again occurred at temperatures lower than those characteristic of the pure salt [3].

3.2. Thermogravimetric measurements

Some thermogravimetric measurements were completed using a Perkin–Elmer TGS-2 (system 4) instrument under non-isothermal conditions heating at 10 K min^{-1}. It was confirmed that the reaction exotherm was accompanied by small weight losses between 680 and 720 K; measured values were 4, 17 and 10% for Mixtures A (0.7), B (1.3) and C (2.5). These include the water weight loss (7.0% of the constituent $CaSO_3 \cdot 1/2H_2O$), representing 2.3, 3.5 and 4.6%, respectively, for the above mixtures. The exotherm is, therefore, accompanied by the evolution of some gaseous products. The later weight loss, above 800 K, is identified as $Ca(NO_3)_2$ breakdown.

3.3. Isothermal kinetic studies using DSC

The exothermic reaction was investigated further by isothermal kinetic studies using the same DSC instrument and in a nitrogen flow (30 cm^3 min^{-1}). Each reactant sample was heated rapidly (100 K min^{-1}) from 323 K to the selected constant reaction temperature: 663, 673, 683 or 693 (±1) K.

Typical isothermal response traces for Mixture B (1.3) are shown in Fig. 6. Fractional reaction (α) values were calculated from the ratios of heat released after selected time intervals to the total heat evolved on completion of reaction [13]. Usually ca. 50 points were used in each numerical integration. Isothermal α–time plots were invariably sigmoid shaped, the representative curves shown in Fig. 7 were calculated from the data in Fig. 6. α–Time values were well expressed by the Avrami–Erofe'ev equation, n=2, [9], between $0.04<\alpha<0.94$ as illustrated by Fig. 8. The calculated activation energy (E) was 235±5 kJ mol^{-1} and the frequency factor (A) was 6×10^{17} min^{-1}. At the lower temperatures studied, the data gave an equally acceptable fit to the same equation with n=3.

Similar isothermal kinetic studies were undertaken for mixtures A (0.7), C (2.5) and D (2.6). Results

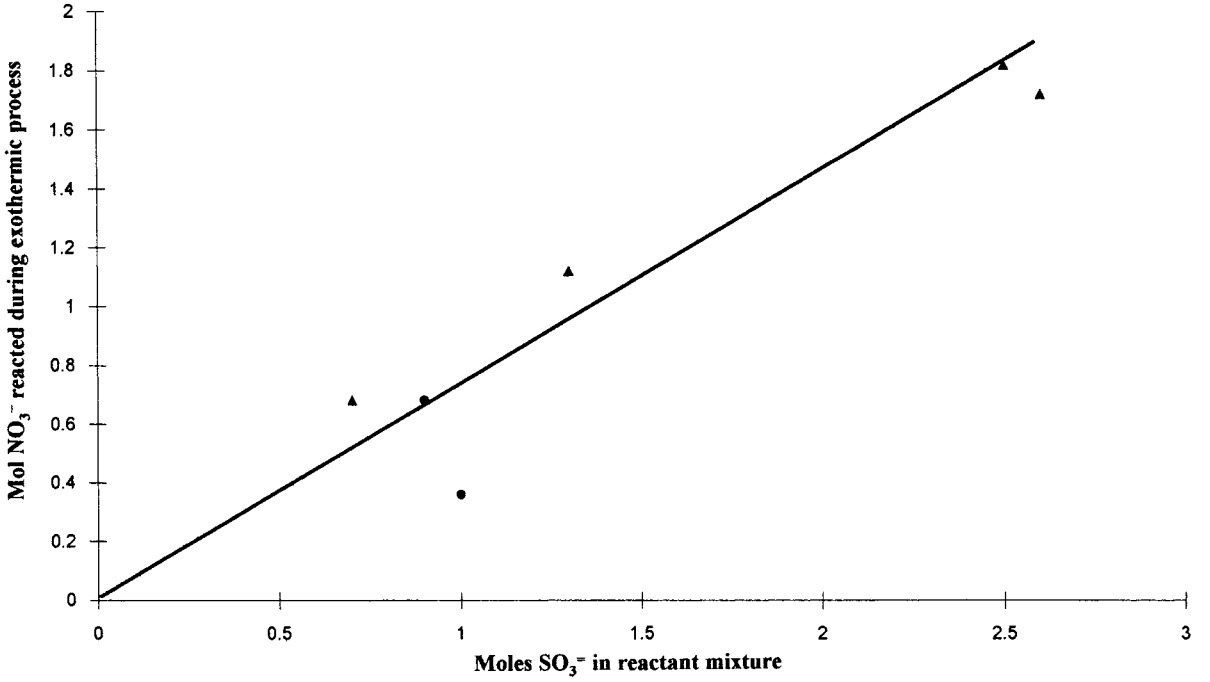

Fig. 5. Plot of amount of NO_3^- (mol) estimated from thermochemical data (Table 1) to have reacted during exothermic rate processes against SO_3^{2-} mol present in the reactant. ●-$CaSO_3 \cdot 1/2H_2O$, ▲ $CaSO_3$ anhydrous.

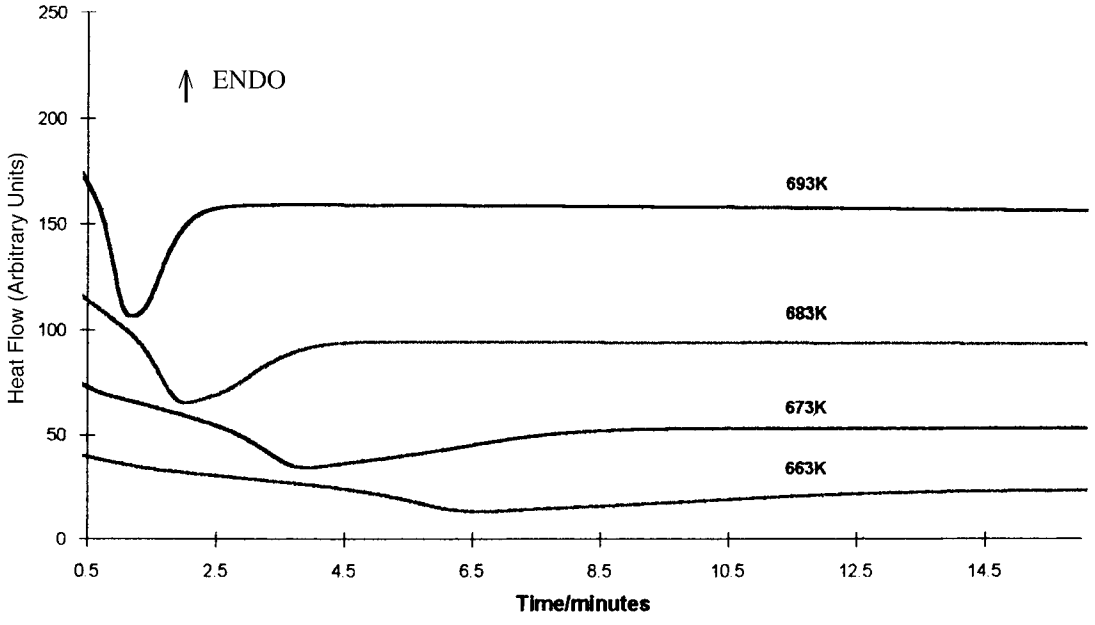

Fig. 6. Typical isothermal DSC response plots for the exothermic reaction in Mixture B (1.3) at 663, 673, 683 and 693 K.

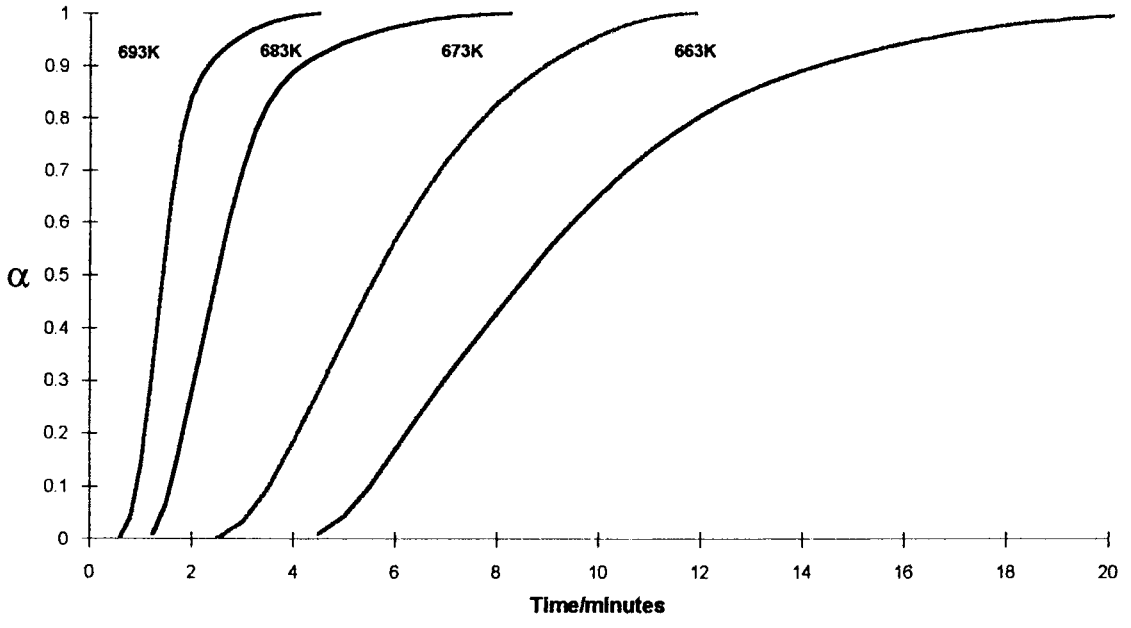

Fig. 7. Sigmoid α–time curves for the exothermic isothermal reaction of Mixture B (1·3) calculated from the data shown in Fig. 6.

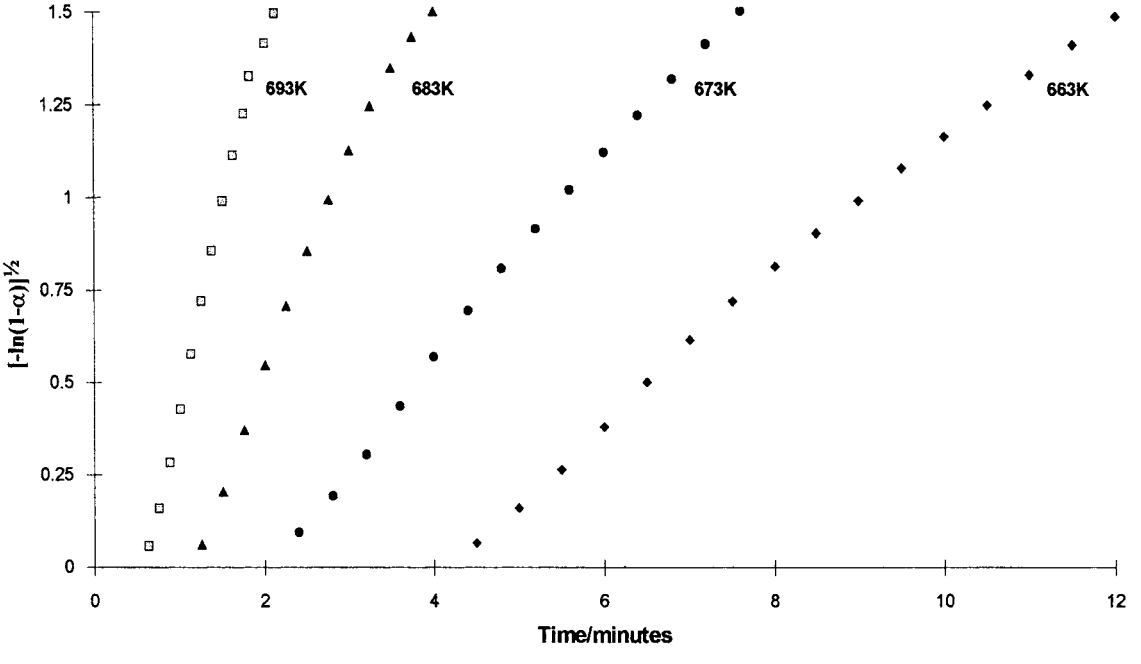

Fig. 8. Avrami–Erofe'ev equation (n=2) [9] plots for data in Figs. 6 and 7.

showed an identical pattern of kinetic behaviour. The Avrami–Erofe'ev equation, n=2, gave the best kinetic representation of the α–time data and calculated values of the Arrhenius parameters were E=226±6, 254±5, 239±5 kJ mol^{-1} and A=5×10^{16}, 2×10^{19} and 3×10^{17} min^{-1}, respectively. All these are regarded as

being in acceptable agreement, identified as due to the same rate process.

A further study showed that Mixture X (0.9) also satisfactorily fitted the Avrami–Erofe'ev equation $n=2$, across a similar α range. For this reactant, containing anhydrous $CaSO_3$, however, the calculated Arrhenius parameters were significantly larger $E=350\pm7$ kJ mol^{-1} and $A=2\times10^{26}$ min^{-1}. Here, the exothermic reaction does not overlap with a concurrent endothermic dehydration.

3.4. Isothermal kinetic studies from gas evolution

Isothermal kinetic studies were based on measurements of the pressures of gas evolved at known times in the constant volume evacuated apparatus. No cold trap was maintained during these reactions. Evolved products are expected to include the water vapour released from $CaSO_3{\cdot}1/2H_2O$ dehydration. Partial analyses of the volatile products were based on pressure changes following the introduction of cold traps, 78 and 178 K.

3.4.1. Mixture B(1.3)

Preliminary comparative experiments showed that α–time curves for the isothermal decomposition of Mixture B (1.3) between 659 and 700 K were acceptably reproducible. Gas evolution proceeded to completion in two overlapping sigmoid-shaped rate processes, illustrated in Fig. 9 for two representative rate ($d\alpha/dt$)–time plots at 659 K.

This partial overlap of consecutive rate processes introduces some uncertainty into the kinetic analyses which, therefore, proceeded as follows. The contributions of the steps were separated by first estimating the pressure corresponding to completion of the first, more rapid, rate process. Separate sets of α–time values were then calculated for each of the two contributing sigmoid-shaped curves and these were subjected to the usual kinetic analysis [9]. It was found, however, that neither rate processes could be acceptably represented by any of the usual rate expressions. Accordingly, reaction rates were calculated from the slopes of the α–time curves, and for each of the separate rate processes, at $\alpha=0.2$, 0.4, 0.6 and 0.8. Values of the activation energy [14] calculated at $\alpha=0.2$ (considered to be the most reliable: other values were always closely comparable) were 177 ± 4 and 169 ± 4 kJ mol^{-1} for the first- and second-rate processes, respectively. These are in most satisfactory agreement with 173 ± 8 kJ mol^{-1} reported [10] for the dehydration of $CaSO_3{\cdot}1/2H_2O$ between

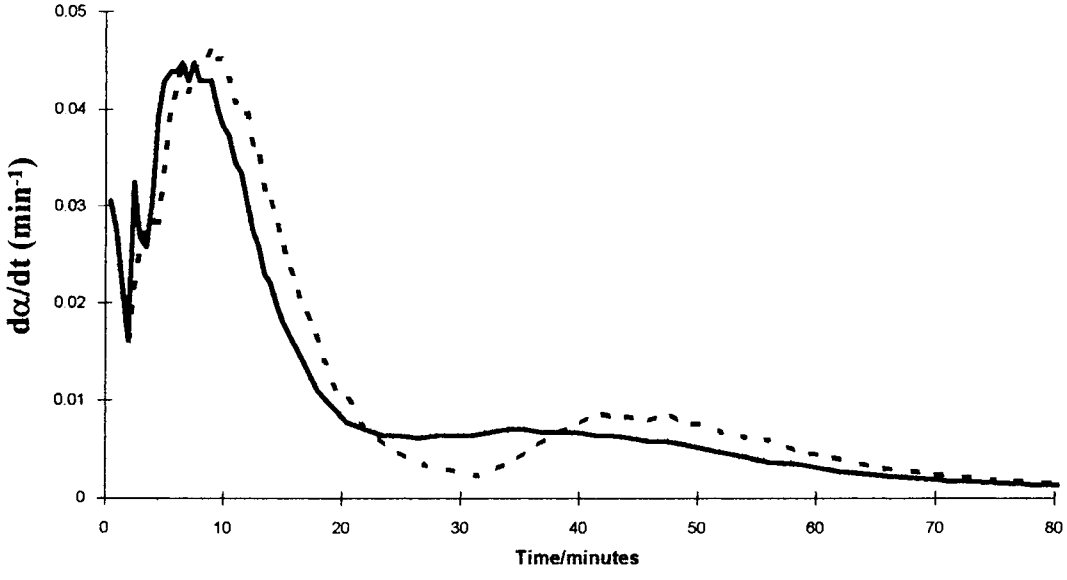

Fig. 9. Plot of reaction rate ($d\alpha/dt$) against time for Mixture B (1.3) at 659 K from evolution of gaseous products in an evacuated constant volume apparatus, for two representative samples.

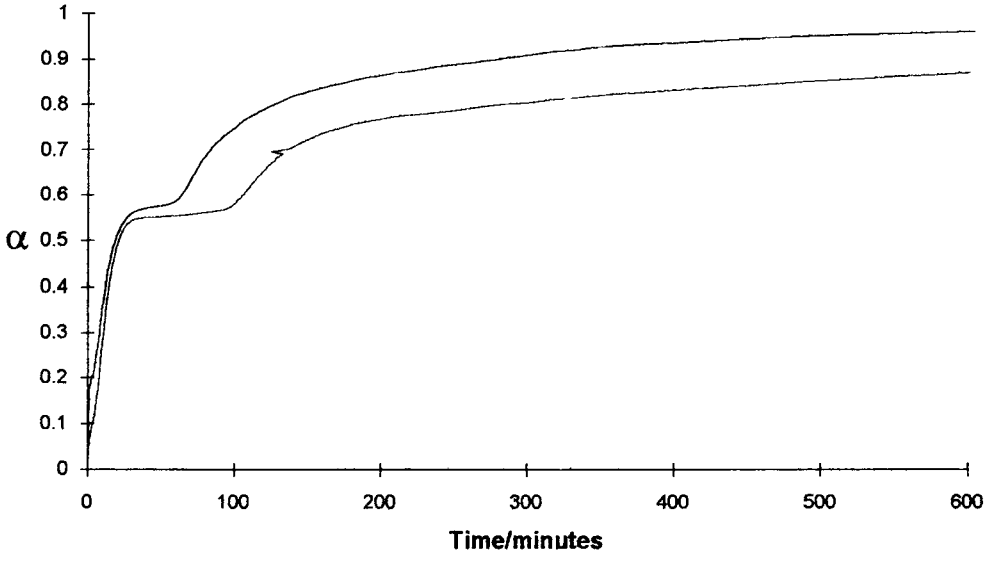

Fig. 10. Typical α–time plots for reaction of Mixture C (2.5) at 651 K from evolution of gaseous products in an evacuated constant volume apparatus.

573 and 673 K. Detailed comparisons, always using identically measured rates ($d\alpha/dt$) from α–time slopes, showed that the first and second reactions studied here proceed at rates that were 0.7 and 0.3 times those for $CaSO_3 \cdot 1/2H_2O$ dehydration at the same temperature. Thus, the dominant gas-evolution process from this mixture can be ascribed to water release from the hemihydrate, perhaps slightly modified by the evolution of other products. The implications of this observation will be discussed further below.

3.4.2. Mixture C(2.5)

The pattern of behaviour characteristic of this reactant was closely similar to that described in the previous paragraph. The only significant difference was that the pressure increases associated with the two rate processes were approximately equal. This is illustrated for two reactions at 651 K in Fig. 10. A conventional kinetic analysis of these separate processes found no satisfactory fit for the usual rate equations [9]. However, again the rates were found, by ($d\alpha/dt$) against α comparisons, to be 0.8 and 0.45 times, those of $CaSO_3 \cdot 1/2H_2O$ dehydration, similar to the observations for the previous reactant.

3.4.3. Mixtures X(0.9) and W(0.6)

These reactants differ from those described above in that the constituent $CaSO_3$ had been previously dehydrated. Rising temperature experiments for Mixture X(0.9) showed that the temperature at which the exotherm occurred for these 'dry' mixtures was increased by ca. 11 K, representing a small diminution in reactivity. α–Time plots for the isothermal gas-evolution reaction between 643 and 666 K were sigmoid-shaped and data satisfactorily fitted the Avrami–Erofe'ev equation, (n=2), Fig. 11. The calculated value of E was 226±13 kJ mol^{-1} and detailed comparisons showed that the reaction rate was significantly less, 0.11 times, than that of $CaSO_3 \cdot 1/2H_2O$ dehydration. A limited number of experiments with Mixture W(0.6) between 646 and 669 K showed closely similar behaviour.

3.5. Partial analyses of products of reactions in vacuum

FTIR examination of the residual products from some of the isothermal decompositions in vacuum identified NO_3^- and SO_4^{2-} as the major constituents

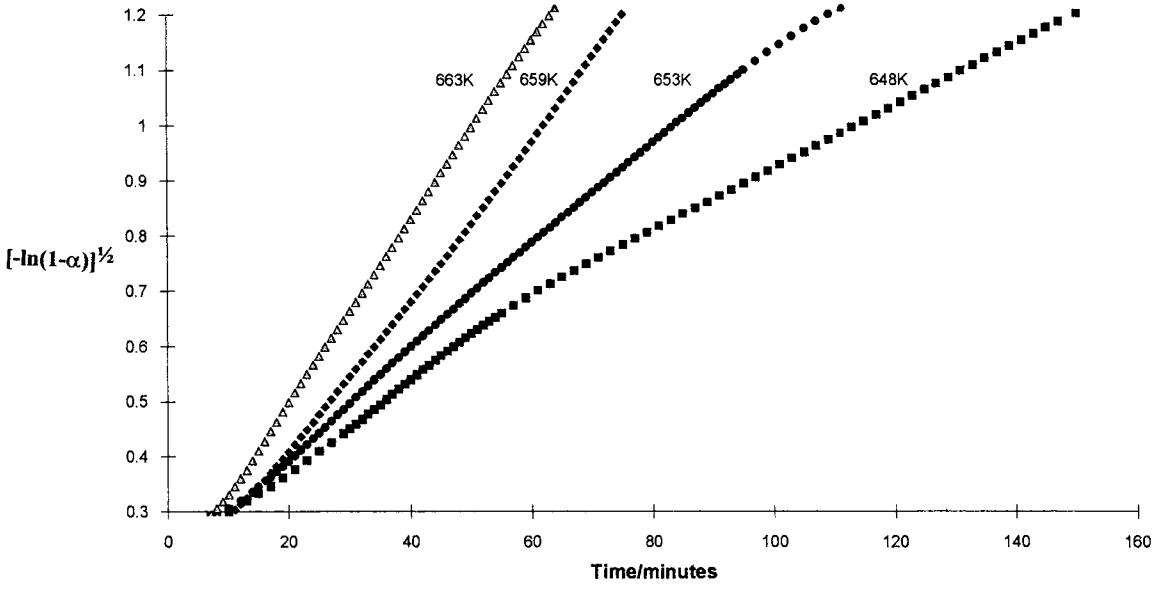

Fig. 11. Avrami–Erofe'ev equation (n=2) [9] plots for reactions of Mixture X (0.9) at 648, 653, 659 and 663 K from evolution of gaseous products in an evacuated constant volume apparatus.

of the residue ($Ca(NO_3)_2$ and $CaSO_4$) but no SO_3^{2-} could be detected.

Partial analyses of the gaseous products were possible using refrigerant traps (see Section 2 above). From these observations, together with the gravimetric data, we estimate that during the exothermic process ca. 0.20±0.10 mol NO and 0.25±0.10 mol NO_2 are evolved from each mol of $Ca(NO_3)_2$ decomposed. The blue colour [15] of the condensate (N_2O_3) confirms the production of both NO and NO_2. Although the water-evolution step ($CaSO_3 \cdot 1/2H_2O$ dehydration) may appear to dominate the rate of gas evolution, secondary or other concurrent chemical changes clearly participate, arising from NO_3^- anion breakdown.

3.6. Electron microscopic examinations of reacted mixtures

Samples of Mixtures A (0.7) and B (1.3) were heated at 10 K min^{-1} in the DSC apparatus in N_2 to the exotherm maximum at 690 K before rapid cooling. The partly reacted salt, α=approx. 0.5, was removed from the containing pan, protected from exposure to the atmosphere and textures were examined in a Jeol 35CF scanning electron microscope. Typical appearances are shown in Fig. 12, these textures are interpreted as providing strong evidence that reactant melting had occurred. Particle boundaries are characterized by rounded surfaces that include the irregular surface features recognized [16] as scars of burst bubbles resulting from escape of gaseous product from within a viscous reactant medium. The aggregation through sintering of powder particles and the absence of crystallographic features, such as flat surfaces, sharp edges and aligned cracks is regarded as strong evidence of melting.

Fusion of this reactant below 690 K was unexpected because the melting point of $Ca(NO_3)_2$ is much higher, 836 K [3]. Reasons for the fusion will be discussed below but here we may note that any liquid present could be local, temporary and within a zone that progresses through the reaction mass as the chemical change advances.

3.7. The reaction mechanism

The reaction studied is an exothermic gas-evolving decomposition arising through interactions of calcium nitrate and calcium sulphite between 650 and 720 K. This occurs close to the temperature of $CaSO_3 \cdot 1/2H_2O$ dehydration and was accompanied by melting.

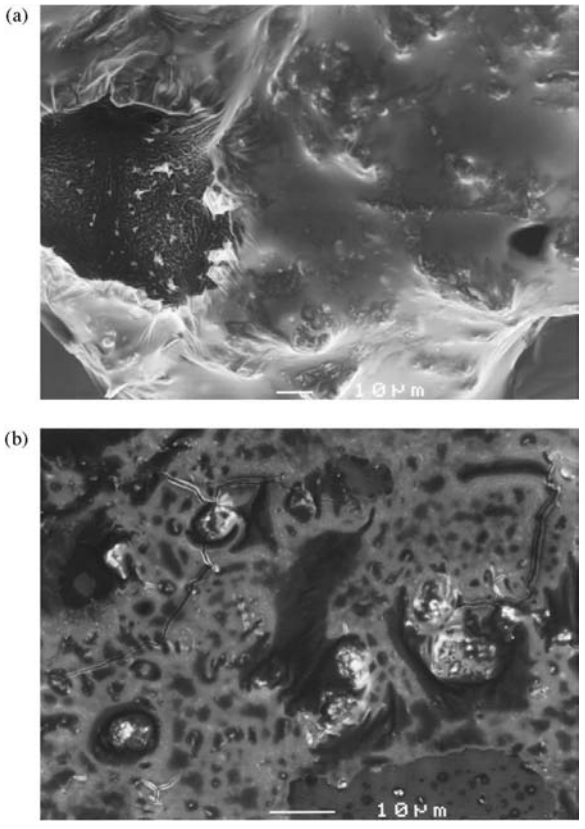

Fig. 12. Representative scanning electron micrographs of Mixture B (1.3) after partial reaction to α=approx. 0.5 (exothermic reaction) at 690 K in N_2. These surface textures confirm the occurrence of extensive melting of the original reactant, crushed to micron-sized particles. (a) The surface of the coherent aggregated material is locally wrinkled. (b) The scarred surface is indicative of bubble evolution following escape of gaseous products from intraparticle reaction. Scale bars both 10 μm.

3.8. Reaction products

The results in Table 1 show that the reaction enthalpy is approximately constant per mole $CaSO_3$ in the mixture. In contrast, the heat evolved increased per mole $Ca(NO_3)_2$ reacted, each 1.0 mol NO_3^- reacted with ≈1.33 mol SO_3^{2-} (see Fig. 5) and the remainder of the $Ca(NO_3)_2$ decomposed at a significantly higher temperature. The extents of these reactions in mixtures, containing anhydrous $CaSO_3$ were less and here due allowance must be made in the thermochemical calculations for the absence of the endotherm from $CaSO_3{\cdot}1/2H_2O$ dehydration [10].

Infrared Fourier Transform Analysis confirmed the presence of sulphate and nitrate but not of sulphite, in the residual products from isothermal reactions below 700 K. The retention of a proportion of the NO_3^- is consistent with the above interpretation of the DSC observations. A search of the relevant thermochemical data [12] leads us to conclude that the only chemical change that is capable of explaining realistically the exothermic process is the oxidation of $CaSO_3$ to $CaSO_4$ by the nitrate. The present observations are explained by the participation of the reaction:

$$Ca(NO_3)_2 + 2CaSO_3 \rightarrow Ca(NO_2)_2 + 2CaSO_4 \quad (2)$$

between 650 and 720 K. The enthalpy of this reaction is estimated [12] to be ≈203 kJ mol^{-1}.

The exotherm response measured is diminished by the concurrent dehydration endotherm from $CaSO_3{\cdot}1/2H_2O$. Assuming a 2/3 overlap, the exotherm expected from reaction (2) is $-203+(2/3)2\times52=-134$ kJ mol^{-1}. This is appreciably larger than the heat released per mole of $Ca(NO_3)_2$ decomposed (Table 1) for Mixtures A (0.7), B (1.3), C (2.5) and D (2.6): calculated values are −72, −82, −116 and −97 kJ mol^{-1}. Thus, the enthalpy change associated with sulphite oxidation is shown to be sufficient to account for the observed exotherms. The value for Mixture Z (1.0), −147 kJ mol^{-1} was larger, in accordance with expectation for the anhydrous reactant, but the value for Mixture X (0.9) was unexpectedly small for reasons that have not been established.

Calcium nitrite is also a potential oxidant, and the heat of a further reaction:

$$Ca(NO_2)_2 + 2CaSO_3 \rightarrow CaO + 2CaSO_4 + \tfrac{1}{2}N_2 + NO \quad (3)$$

may contribute 245 kJ mol^{-1} to the exotherm [12]. Alternative sulphite oxidation reactions include, for example:

$$Ca(NO_3)_2 + 3CaSO_3 \rightarrow CaO + 3CaSO_4 + 2NO \quad (4)$$

The calculated enthalpy change, −108 kJ mol^{-1}, is however too small to account for the observed exotherm. The decomposition of calcium nitrite is endothermic, −234 kJ mol^{-1}, for:

$$Ca(NO_2)_2 \rightarrow CaO + NO + NO_2$$

It is already accepted in the literature that the breakdown of $Ca(NO_3)_2$ is complicated, involving several concurrent and interlinked reactions that probably include [3,17–19]:

$$Ca(NO_2)_2 \rightarrow CaO + 2NO + \tfrac{1}{2}O_2$$

$$Ca(NO_2)_2 + 2NO_2 \rightleftharpoons Ca(NO_3)_2 + 2NO$$

In interpreting the present data, therefore, we conclude that several chemical processes may contribute to the exothermic reaction at ca. 700 K. The heat released is attributable to sulphite oxidation ($\rightarrow SO_4^{2-}$) but a number of additional chemical changes may participate, including the interconversions of NO_2^- and NO_3^-. The balance between these contributing rate processes may also vary systematically with reaction conditions, such as temperature, prevailing gas pressures, mixture composition, etc. Observations on the overall process are insufficient to elucidate the detailed mechanism including the extents of all the reactions involved [20]. Thermochemical observations for the exotherm are subject to uncertainty because of the effect of this process in modifying the subsequent $Ca(NO_3)_2$ decomposition endotherm. Uncertainties are thereby introduced into the estimations of the amounts of NO_3^- and NO_2^- participating in both the stages, Table 1.

Some oxides of nitrogen are formed during the exothermic reaction. This is shown by the small weight loss at ca. 700 K, detected in the thermogravimetric studies (in addition to that due to dehydration). The partial analysis of the gaseous products from the isothermal studies confirm that the reaction produces NO and NO_2 in approximately equimolar amounts. That proportion of $Ca(NO_3)_2$ decomposed during the reaction with $CaSO_3$ can be expressed by

$$Ca(NO_3)_2 \rightarrow CaO + NO + NO_2 + 2[O]$$

where [O] is used in sulphite oxidation. The heat of this reaction is, however, insufficient to account for the exotherm.

3.9. Reactant melting

The formation of $Ca(NO_2)_2$, shown in reaction (2), explains the early liquefaction during reactions of the present mixtures because the melting point of calcium nitrite has been reported as 551 K [19]. It is also known [17–19] that $Ca(NO_2)_2$ decomposition is accompanied by $Ca(NO_3)_2$ formation. Thus, the production of nitrite in mixtures is expected to result in the appearance of a liquid phase that may be local and temporary, but in which reaction proceeds more readily. Fusion is accompanied by the relaxation of intracrystalline stabilizing forces and an increase in reactant mobility, both of which can increase reactivity [21]. The melt phase is expected to contain NO_3^-, NO_2^-, SO_3^{2-} and possibly some SO_4^{2-}. The sulphite oxidation process is identified as being dominant, but is accompanied by some decomposition of both NO_3^- and NO_2^-.

3.10. Significance of $CaSO_3 \cdot 1/2H_2O$ dehydration

The occurrence of the exothermic reaction described above at almost the same temperature as $CaSO_3 \cdot 1/2H_2O$ dehydration suggests a direct association between these rate processes. Comparisons of the isothermal kinetic studies confirmed the very close relationship between the rates of $CaSO_3 \cdot 1/2H_2O$ dehydration [10] and the reaction of these mixtures, Fig. 13. This can be explained by participation of the water vapour released in the above reactions, perhaps involving the production of HNO_3 by the hydrolysis of $Ca(NO_3)_2$. Such mechanistic proposals will not change the overall thermochemical considerations presented because above 700 K both nitric acid [15] and $Ca(OH)_2$ [22] dissociate.

Under isothermal conditions, the exothermic reaction below 700 K proceeded to completion in two consecutive rate processes. While the evidence available here does not enable a final explanation for this behaviour to be provided, the following model satisfactorily accounts for the observations. The decomposition of $Ca(NO_3)_2$ has been identified as a stepwise reaction [3]. In the present system, the oxidation of sulphite ($\rightarrow SO_4^{2-}$) by nitrate or by nitrite may proceed at different rates. We also note that reactions in mixtures containing the anhydrous sulphite occurred at a somewhat slower rate (0.1 times) or at a slightly enhanced temperature. This could be due to the participation of only a small amount of more strongly retained water in these mixtures. Alternatively, it could be due to enhanced reactivity associated with a structural reorganization of the anhydrous $CaSO_3$ in

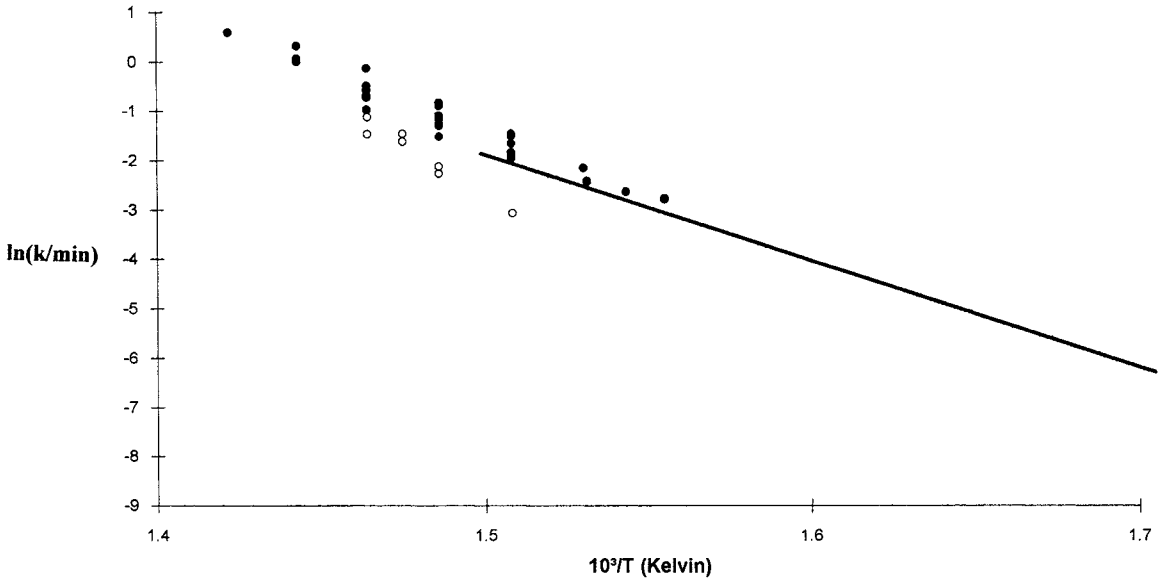

Fig. 13. Arrhenius plot comparing rates (from $d\alpha/dt$) at $\alpha=0.2$) of the following reactions: $CaSO_3 \cdot 1/2H_2O$ dehydration [10], line; $Ca(NO_3)_2 \cdot xH_2O + CaSO_3 \cdot 1/2H_2O$ reactant mixtures (●); $Ca(NO_3)_2 + CaSO_3$ anhydrous reactant mixtures (O).

the vicinity of the dehydration temperature, the Hedvall Effect [23].

The sigmoid shaped α–time plots for the isothermal reactions (Figs. 7 and 10) may be due to effective control by $CaSO_3 \cdot 1/2H_2O$ dehydration [10], a result that is supported further by the close similarity of E values as well as reactivity, Fig. 13. Such autocatalytic behaviour may also be expected in a reactant undergoing progressive melting [21]. This, of course, is a real possibility for reaction in the mixture which contains a small proportion of water.

3.11. Mechanistic conclusions

The present study has investigated an exothermic reaction between calcium nitrate and calcium sulphite accompanied by melting, between 650 and 720 K. Onset of reaction is probably promoted by the water released by $CaSO_3 \cdot 1/2H_2O$ dehydration. The heat release is ascribed to sulphite to sulphate oxidation with the probable dominant participation of reactions (2–4). These overlap with the dehydration endotherm and reaction is accompanied by NO_3^- and NO_2^- decompositions. The overall chemical changes undoubtedly include contributions from other participating rate processes, the extent of which may vary somewhat with reaction conditions including temperature, contact with product gases and mixture composition.

An interesting result is the demonstration that sulphite oxidation proceeds at a lower temperature and to a larger extent than readily occurs [1,2,7] during calcium sulphite oxidation (1). It is concluded that during reactions in the liquid/melt no product barrier layer of $CaSO_4$ is developed that progressively opposes sulphite oxidation.

The melting and decomposition of all excess calcium nitrate remaining in the present mixture occurred at temperatures somewhat below those characteristic of the pure salt. This is ascribed to promotion of the decomposition by small amounts of products from the exothermic process, probably including nitrite, that may appreciably accelerate nitrate breakdown [3].

3.12. Relevance of the present observations to environmental protection

Our work in this field [3,8] was prompted by the necessity to extend chemical knowledge of the thermal properties of $Ca(NO_3)_2$ under conditions that relate to the possible participation of this intermediate in flue-gas denitrification and desulphurization

[1,2,7]. It is known [3,17–19] that NO_2 and NO react with $CaCO_3$ and/or CaO to form calcium nitrate, which may therefore have a transitory existence under the conditions in which calcite is used [2,7] for coal combustion volatile product treatments. The present work provides evidence that $Ca(NO_3)_2$ is an intermediate capable of promoting $CaSO_3$ oxidation, identified [2] as the slow step in the sulphation reaction (1). The participation of reactions involving intermediate melt formation appear to offer some potential for increasing the efficiency and effectiveness of calcium compounds in removing the acid rain precursors from flue gases. It may be that both denitrification and desulphurization treatments could be combined through the direct or indirect use of combustion product NO_2 in the oxidation of $CaSO_3$ during a low-temperature sulphation reaction. Development of this approach requires further work designed to exploit the enhanced reactivity in the molten phase, 600–700 K. The products are expected to contain calcium nitrite (soluble and of possible value as a fertilizer) and calcium sulphate (insoluble and used in plaster board manufacture).

It could be useful to investigate the efficiency and effectiveness of nitrate-containing mixtures in low-temperature desulphurization reactions. This approach could study the reactions of SO_2 with $Ca(NO_3)_2$, possibly $Ca(NO_2)_2$ and mixtures containing $CaCO_3$, $Ca(OH)_2$ or $Ca(NO_3)_2$ with a cheap nitrate, such as NH_4NO_3. The higher cost of the reactant would be off-set by the greater removal of the pollutant.

References

[1] D.C. Anderson, Ph.D. Thesis, The Queen's University of Belfast, 1994.
[2] D.C. Anderson, P. Anderson, A.K. Galwey, Fuel 74 (1995) 1018, 1024 and 1031.
[3] C.A. Ettarh, Ph.D. Thesis, The Queen's University of Belfast, 1995; C.A. Ettarh, A.K. Galwey, Thermochim. Acta 288 (1996) 203.
[4] G. Gut, M.J. Abd-Ellatif, A. Guyer, Helv. Chem. Acta 45 (1962) 506.
[5] D. Bourgeois, P. Zecchini, D. Devin, C.R. Acad. Sci. Paris, Ser. C 278 (1974) 53.
[6] E. Gimzewski, S.H. Hawkins, Thermochim. Acta 99 (1986) 379.
[7] D.C. Anderson, A.K. Galwey, Proc. R. Soc. London A452, 1996, p. 585, 603.
[8] C.A. Ettarh, A.K. Galwey, Thermochim. Acta 261 (1995) 125.
[9] M.E. Brown, D. Dollimore, A.K. Galwey, Comprehensive Chemical Kinetics, vol. 22, Elsevier, Amsterdam, 1980.
[10] D.C. Anderson, A.K. Galwey, Canad. J. Chem. 70 (1992) 2468.
[11] N.J. Carr, A.K. Galwey, Proc. R. Soc. London A404 (1986) 101.
[12] R.C. Weast (Ed.), CRC Handbook of Chemistry and Physics (many editions), CRC Press, Boca Raton, Florida.
[13] M.E. Brown, A.K. Galwey, A. Li Wan Po, Thermochim. Acta 220 (1993) 131; 203 (1992) 221.
[14] M.E. Brown, A.K. Galwey, Anal. Chem. 61 (1989) 1136.
[15] N.V. Sidgwick, The Chemical Elements and their Compounds, vol. 1, Clarendon, Oxford, 1950, p. 687.
[16] S.D. Bhattamisra, G.M. Laverty, N.A. Baranov, V.B. Okhotnikov, A.K. Galwey, Phil. Trans. R. Soc. London A341 (1992) 479.
[17] M. Doumeng, Rev. Chim. Miner. 7 (1970) 897.
[18] S.B. Warrington, P.A. Barnes, E.L. Charsley, Proc. 2nd ESTA, Hyden, London, 1981, p. 315.
[19] S.B. Warrington, Ph.D. Thesis, Leeds Polytechnic, 1983.
[20] A.K. Galwey, L. Pöppl, S. Rajam, J. Chem. Soc., Faraday Trans. I 79 (1983) 2143.
[21] A.K. Galwey, J. Thermal Anal. 41 (1994) 267; Drug Stability 1 (1995) 3.
[22] A.K. Galwey, G.M. Laverty, Thermochim. Acta 228 (1993) 359.
[23] V.V. Boldyrev, M. Bulens, B. Delmon, The Control of the Reactivity of Solids, Elsevier, Amsterdam, 1979, p. 32.